Key Engineering Materials
ISSN: 1662-9795, Vol. 1047, pp 313-323

Submitted: 2026-01-20
Accepted: 2026-02-11
Online: 2026-04-13

Measurement of Forces Generated during Robotized Additive Manufacturing Process Using Pellet Extruder

Salah-Eddine Ouassil[1,a*], Pascal Casari[2,b], Élodie Paquet[3,c], Guillaume Racineux[1,d]

[1]Nantes Université, Ecole Centrale de Nantes, CNRS, GeM, UMR 6183, 44321 Nantes, France

[2]Nantes Université, Ecole Centrale Nantes, CNRS, GeM, UMR 6183, F-44600 Saint-Nazaire, France

[3]Nantes Université, Romas Team, LS2N UMR CNRS 6004, 44475 Carquefou, France

[a*]salah-eddine.ouassil@ec-nantes.fr, [b]pascal.casari@univ-nantes.fr, [c]elodie.paquet@univ-nantes.fr, [d]guillaume.racineux@ec-nantes.fr

Keywords: additive manufacturing, interlayer bonding, pellet-extrusion, forces measurement.

Abstract. Robotic additive manufacturing using pellet extrusion has gained significant scientific interest and industrial maturity. Increased part dimensions, reduced production time, and lower raw material costs are the main advantages of this process. This development has led to a strong demand for improved control and understanding of the process and of multiple phenomena occurring during fabrication. Consequently, process monitoring has received considerable attention, as it enables better understanding and detection of anomalies and their origins during manufacturing, allowing for immediate correction when possible or for more in-depth post-process analyses. Several studies in the literature have focused on monitoring parameters such as extrusion temperature, layer height, and printing speed to investigate their effects on final part quality and mechanical performance. In the present study, the objective is to quantify the forces applied to the deposited material during robotic additive manufacturing by pellet extrusion. This is made possible using a six-component force sensor, which allows the measurement of forces and moments along the three directions (X, Y, and Z). Following data acquisition, the results allowed understanding of force variations throughout the fabrication cycle and their correlation with the different stages of the manufacturing process. A single layer curve was explained with the corresponding peaks of each segment of the trajectory. It was found that at rounds there are peaks in Z forces due to the fact that, at the rounded sections, there is a slight accumulation of material, as the robot's travel speed decreases while the material flow rate remains constant. This therefore results in higher applied forces. Consequently, it was observed that from the third layer onward, forces along the Z direction were almost no longer detectable. These measurements aim to facilitate the detection of manufacturing defects through unexpected force variations and to relate these observations to the final mechanical properties of the fabricated parts.

Introduction

Additive Manufacturing (AM) is a revolutionizing process that represents many pros compared to conventional manufacturing methods. In fact, AM, also known as 3D printing, consists of joining material layer upon layer till obtaining the final part [1]. Remarkable precision, high adaptability and the ability to fabricate complex geometries are some of the advantages offered by AM technologies [2], [3]. Many industries are more and more adopting the AM process [4], such as aerospace, medicine and automotive [4]. Fused Filament Fabrication/Fused Deposition Modeling (FFF/FDM) is one the most widely used technologies of AM as it is affordable and easy to use [1], [2], [5]. It consists in heating a filament material above its melting temperature then extrude it through a nozzle and deposit it onto a build plate.

Large choice of materials exists in FDM to respond to different mechanical and functional requirements. Usually, the low-temperature thermoplastics are the most used materials as they are affordable and sufficient for non-critical applications, like demonstration parts [6]. Recently, more materials such as engineering materials are present in the market for different applications. Moreover,

reinforced plastics also entered the race as their incorporation showed remarkable improvement in structural, thermal and mechanical properties [7] . Besides the material, the impact of manufacturing parameters such as layer height, printing speed and infill density on the quality of the final part was investigated in several studies [8]–[10]. Despite all the interest and evolution, limited fabrication dimensions and low production flow restricted the use of this technology by large scale industry.

To deal with these restrictions, a combination of two solutions was revealed. The first solution consists of developing a new technology of material extrusion process of pellets instead of filament. Arburg company has launched in 2015 the Arburg Plastic Freeforming (APF) where the plastic granulate is melted and then extruded [11], [12]. With this technique, also called "Fused Granulate Fabrication (FGF)", production times can be reduced by up to 200 times because of the direct feeding of pellets [13], thus the cost of the raw material can be reduced by more than 10 times compared to FFF [5], [14]–[17]. The second solution to overcome some FDM restrictions is the use of multi-axis platforms instead of Cartesian coordinate systems. Conventionally, extrusion-based AM machines use three-axis coordinate system [18], [19]. It is widely used thanks to its simple mechanisms and simple process flow. However, this system has limitations. When the object is more complex, the need of support structures, staircase effect due to planar layer-by-layer manufacturing, and high machine frame dimensions compared to the fabrication volume are some of these shortcomings [18]–[20].

Therefore, multi-axis AM platforms have been developed to address these limiting factors using robot arms. Either for polymer- or metal-based AM technologies, this 6 degree-of-freedom (6DOF) solution gained interest from the 3D printing community [19]. These systems offer similar floor occupancy as the cartesian 3-axis ones but the kinematics lead to an increased fabrication volume [21]. For this reason, and in order to accelerate the production rate, many leading manufacturers and research laboratories in AM field adopted robotic-based systems.

Although extrusion-based AM techniques has known developments and increased interest from researchers and industries, the process still needs more understanding and in-depth control during the process. Hence, several studies justified the need of monitoring in order to discern the impact of numerous factors on the fabrication. In a review conducted by A. Oleff et al. [22], they gathered many studies of material extrusion process monitoring. The choice of studies was made following many criteria. One of them was the sensor technology used depending on what parameter the paper was interested to monitor. As a result, it has been shown that only 2.6% of the total number of sensors used in several studies was used for force/pressure monitoring. In addition, they reported that these forces sensors were mostly used to inspect the feeding system and the extrusion head [22]. Other sensor technologies were about temperature, vibration, 2D vision, 3D vision, etc.

Quality control through process monitoring can be utilized in different AM technologies for various materials such as polymers and concrete. For this latter, Barry et al. [23] measured the force exerted by the print head on the material extruded. They proceeded to the instrumentation of the extrusion nozzle with load cells to achieve real-time quality control. This approach helped them correlating between the forces of the extruder nozzle and the material hardening process and its impact on the printing quality. In other studies, most force sensors were used to measure extrusion forces and pressure generated by the melting process. The load cell in the cited studies was generally located between the extruder and the hot end to acquire force data of the extrusion process [24]–[27]. In this position, the load cell records movement axis acceleration and vibrations.

For our study, the aim is to quantify the total forces, external to the extruder, that are applied on the deposited material and correlate them to the printing steps. Parts were designed and subsequently fabricated while the forces are measured by the sensor. The resulted data was then analyzed and explained.

Material and Method

Material

In our case, the Dahltram T-100GF pellets from Airtech are used. It is a thermoplastic material reinforced with 30% of glass fibers. It has a maximum temperature use of 65 °C and a heat deflection temperature (HDT) of 70 °C. Mechanical properties of the material are given in Table 1. In addition, Differential Scanning Calorimetry (DSC) analysis was conducted in order to identify thermal transitions in the material such as glass transition (Tg), melting temperature (Tm) and crystallization properties if there is any. Analysis was performed using DSC 200 F3 Maia from NETZSCH. As-received- and printed samples of 10 – 15 mg have been tested in a temperature range from -10 °C to 270 °C at a heating and cooling rate of 20 °C/min. During the tests, nitrogen gas was injected at a flow rate of 50 ml/min as a protective gas of both measurement cell and sample.

Table 1. Material properties given from the manufacturer.

Composition and thermal properties	Values	Mechanical properties	Values
Reinforcements	Glass Fiber	Tensile Strength (X-direction)	79.3 MPa
% Fiber loading	30%	Tensile Strength (Z-direction)	25.9 MPa
HDT	70 °C	Tensile Modulus (X-direction)	6.6 GPa
Use Temperature	65 °C	Tensile Modulus (Z-direction)	3.7 GPa

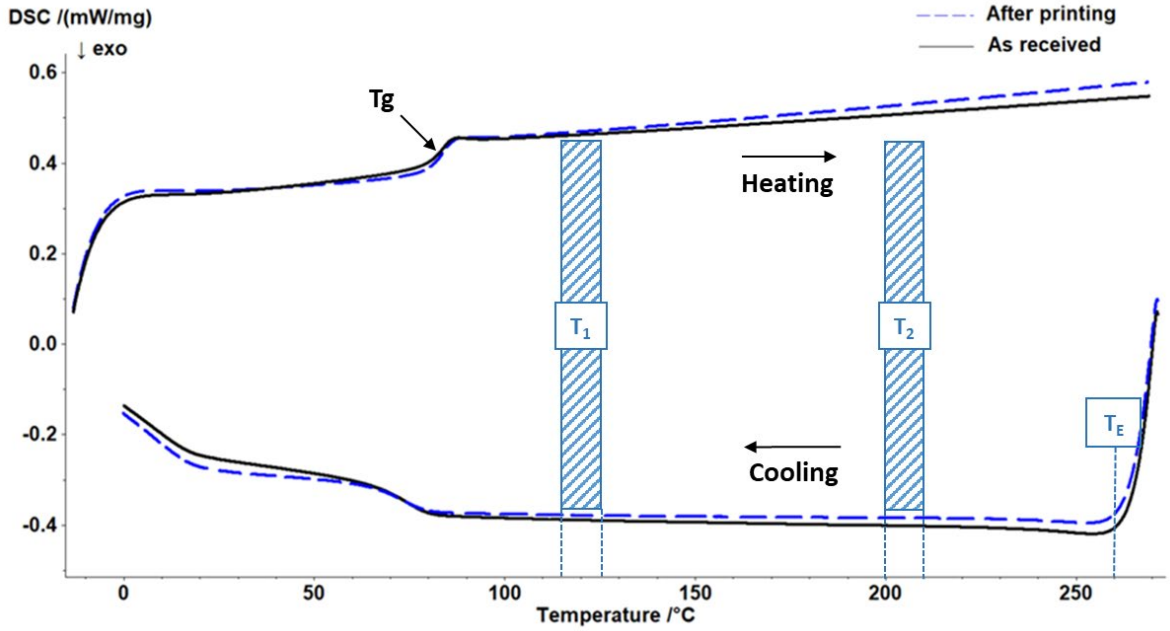

Fig. 1. DSC thermograms of as-received and printed glass fiber reinforced PETG, with key process temperatures discussed subsequently.

The results in Fig. 1 showed no cold crystallization or melting peaks. This is due to the amorphous nature of PETG [28], which was not impacted by the presence of glass fiber reinforcements. The glass transition temperature detected is around 80 °C, which is quite the same with references studying the same neat material [28], [29].

For more information about the material, dimensions of the pellets (Fig. 2) and glass fibers were measured. A Keyence VHX-7000 digital microscope with integrated 2D/3D measurement was used to determine fibers dimensions. For pellets dimensions, they were quantified using a caliper. The dimensions of both, pellets and fibers are similar to the most industrial materials dimensions commercialized in the market. As for fibers, the diameter measured is 13 µm, which is consistent with the commonly used value by manufacturers (10 µm – 20 µm). As for pellet diameter, the value found is around 3 mm, which is also coherent with the existing values that indicate a diameter between 2 mm and 5 mm.

Fig. 2. Image of pellets of the material used for this study.

Method

Experimental setup

A 6-axis robot-based additive manufacturing system equipped with a pellet-extrusion head was employed. The robotic arm used is a TX160L from Stäubli, featuring a repeatability error of ±0.05 mm, ensuring accurate control of trajectories and printing parameters.

The extrusion head, an E25 model from CEAD, provides a deposition rate of up to 12 kg/h and can reach an extrusion temperature of 400 °C.

Data collection

During the manufacturing process, the HBK MCS10 multi-axis sensor was used to measure the forces applied by the extrusion head. It has the ability of measuring up to 6 different forces and moments simultaneously with an accuracy class of up to 0.1.

The forces data was recorded by a 16-channel Bridge Amplifier MX1615 from HBM. It was wired from one side to a laptop equipped with Catman Data Acquisition Software, and to the load sensor from the other side.

For thermal monitoring, it was conducted using a Flir One Edge PRO thermal camera. It allows an object temperature range from 0 °C to 400 °C with a thermal resolution of 19,200 pixels. Two different live spots measurement were used for this study (Fig. 5). Thermal analysis showed a temperature drop of 40 – 45 °C at the moment of extrusion (T_E-T_2 in Fig. 1), knowing that the extrusion temperature is T_E=255 °C. It was found that, with a layer time of 109 seconds, the temperature of the previous layer at the moment of the new layer deposition is between 115-120 °C (T_1 in Fig. 1), which represents 135 °C decrease from the extrusion temperature.

For further analysis and documentation, fabrications were recorded using professional camera. The complete experimental setup is presented in Fig. 3.

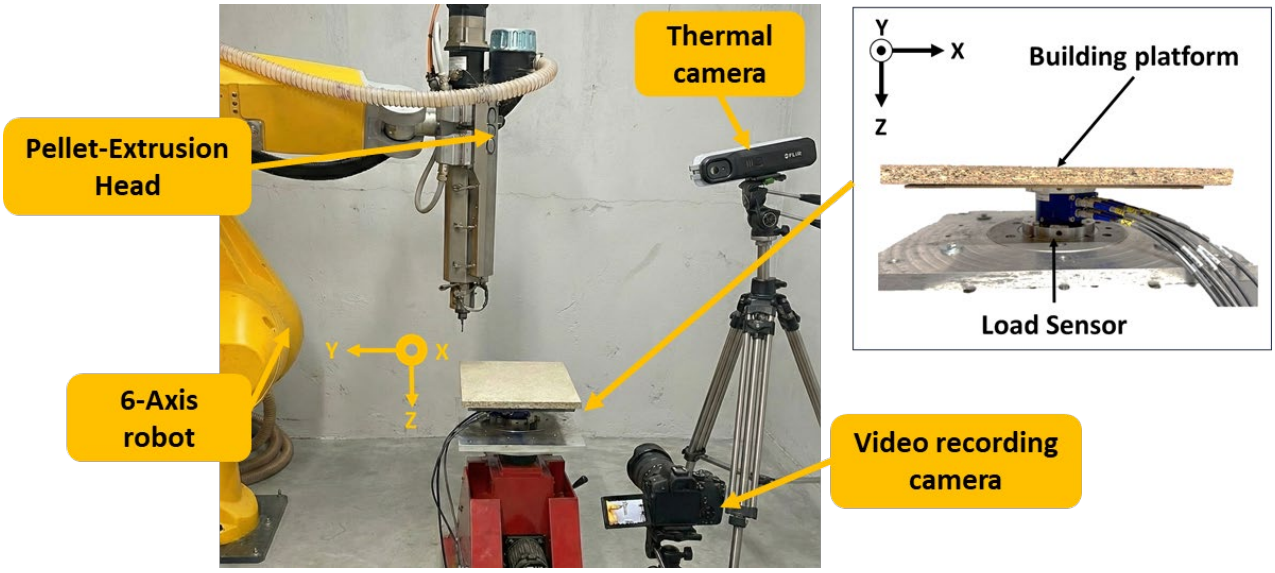

Fig. 3. The setup used for the experiment.

As the objective of this study does not expect variations of the processing parameters, the manufacturing parameters chosen are the same recommended by the material manufacturer and the extrusion head supplier. These parameters are summarized in Table 2.

Table 2. Parameters used for additive manufacturing of the part.

Parameters	Layer height	Speed	Nozzle diameter	Flowrate	Layer width
Values	3 mm	25 mm/s	6 mm	7 kg/h	11-12 mm

Results and Interpretation

To quantify the forces generated during robotic additive manufacturing using pellet extrusion, a dedicated part was designed to enable the extraction of the maximum amount of relevant data, in accordance with the objectives of the measurements. Consequently, a part including trajectory variations in both the X- and Y-axis directions was selected and designed with dimensions matching the build platform used. The geometry of the part and its dimensions are shown in Fig. 4.

The experimental campaign began with preliminary tests to verify the hardware and software of the setup. This validation included leveling the support/build-plate assembly, ensuring that the force sensor accurately measures loads along the three axes, and confirming proper material extrusion. Once testing and verification were successfully completed, the part was fabricated. Additional fabrication trials are planned to ensure repeatability and to establish a dataset. The part after fabrication is shown in Fig. 4. At the end of the additive manufacturing process, and measurements in parallel, the collected data was processed and plotted using a Python-based code. The raw force curves along the three axes (Fx, Fy, Fz) are shown on Fig. 6. Torques were neglected in this initial phase of the study. The time axis of the plots corresponds to the total fabrication duration in seconds.

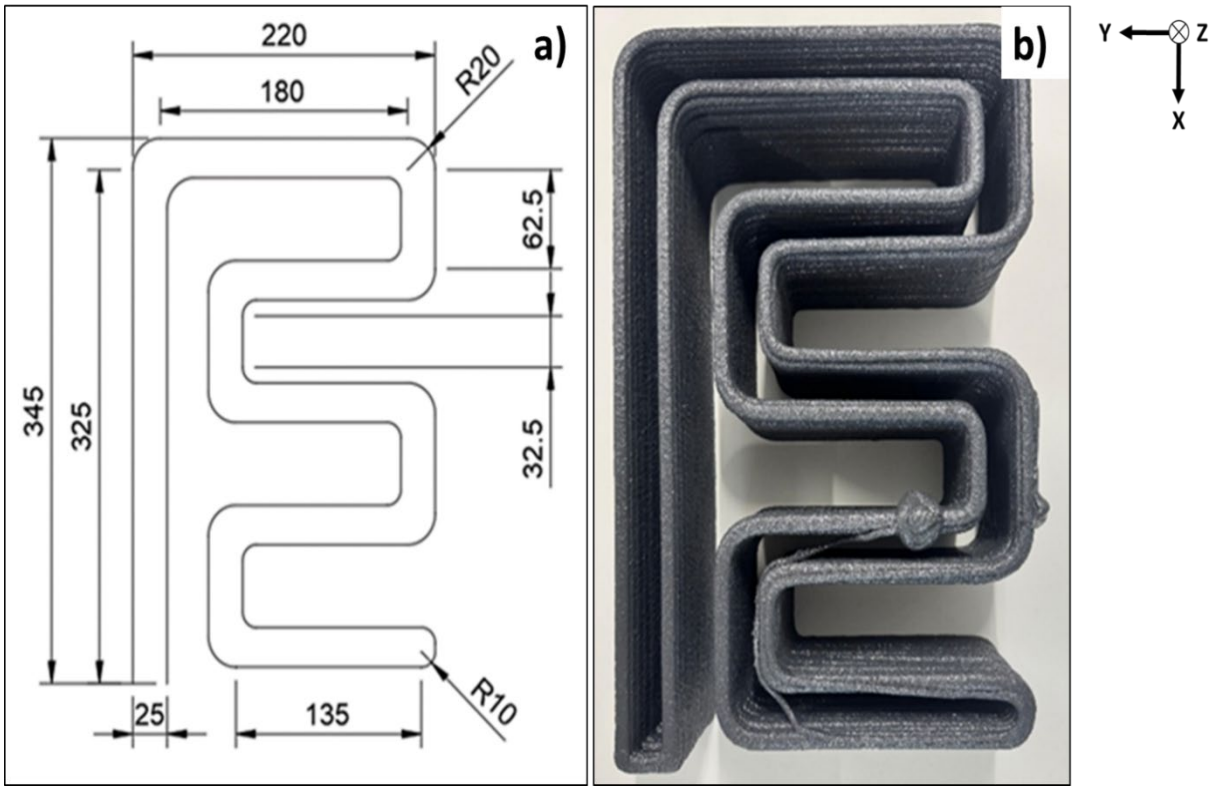

Fig. 4. a) Part design dimensions in mm and b) part after fabrication.

Initially, a significant decrease, or even an absence, of applied force was observed after approximately 230 s of fabrication. For the first layer, the forces are higher as layer height was reduced (2.5 mm) to ensure a strong adhesion with the fabrication bed. This led to a compressed layer, resulting in an increased layer width that was observed via the microscope as shown in Fig. 8b. Besides the first layer, the layer height was 3mm. The evolution of the Fz curve is linear, indicating a constant extrusion rate. The evolution in the Z-axis force (Fz) is related to the cumulative mass of the deposited material throughout the fabrication process. In contrast, the forces along the X- and Y-axis exhibit minimal amplitudes over the entire measurement period.

For more detailed analysis of the force curves, a 1 Hz low-pass filter was applied to remove noise that could disturb proper interpretation of the data. Hence, all the following curves presented are filtered.

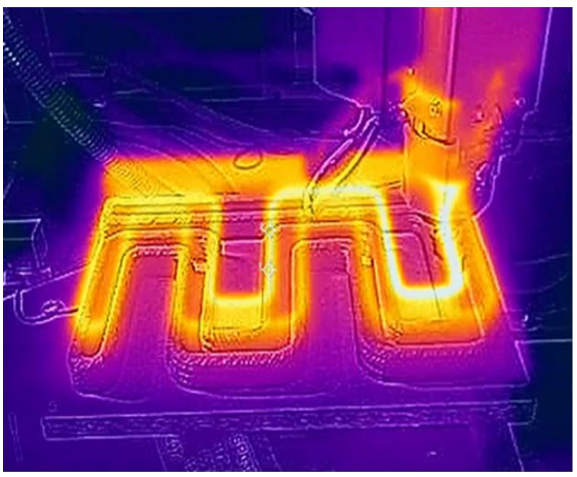

Extrusion temperature : **T_E = 255 °C**
Previous layer temperature at the moment of deposition : **T_1 = [115 °C - 120 °C]**
Material temperature at the nozzle exit : **T_2 = [200 °C – 210 °C]**

Fig. 5. Thermal monitoring during fabrication and key process temperatures measured.

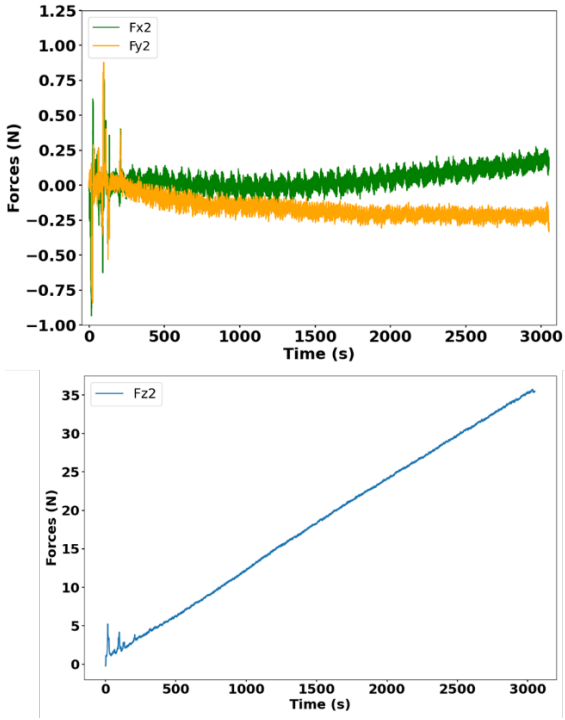

Fig. 6. Forces curves following X, Y, and Z sensor's axes.

For a better understanding of the force curves and their interactions during the additive manufacturing process, the toolpath of the first layer of the part was divided into segments (Fig .7). It should be noted that the total duration of a single layer is 109 seconds. The segments are labeled from A to V in the order of fabrication. The purple marker on both the toolpath and the force curves indicates the actual starting point of the additive manufacturing process of the part. On the graph, each portion of the curve corresponding to a segment is separated by dashed lines, with the segment reference indicated. The regions corresponding to circular features on the curves are highlighted. The corners are characterized by a change in the X- and Y-axis directions and by a peak in the Z-axis force.

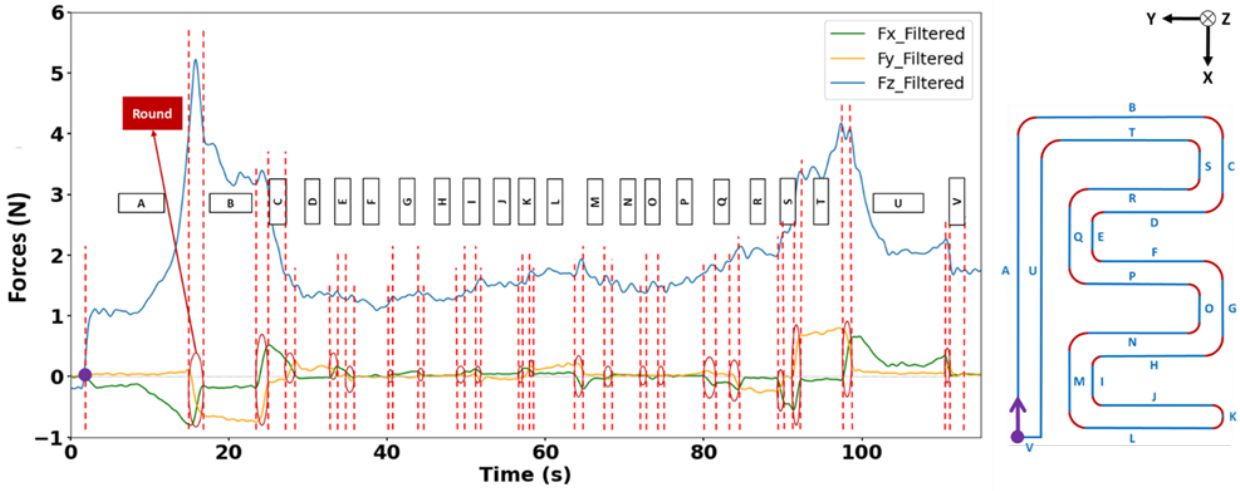

Fig. 7. Force curves measured along X, Y, and Z sensor's axes during the fabrication process, with correspondence between the different stages of the toolpath and their respective segments of the curves.

At the starting point, a clear and immediate increase in Fz is observed, followed by a relative stabilization corresponding to segment A. As the trajectory approaches the first corner, the force increases and reaches a peak due to the robot deceleration while maintaining a constant material flow rate. This pronounced peak can be explained by imperfect horizontality/flatness of the build platform, resulting in the extrusion head being positioned very close to the platform and therefore inducing

higher applied forces. When transitioning to segment B, a change in direction is detected through a sign change on Fx and Fy : segment A corresponds to motion along the −X direction, whereas segment B corresponds to motion along the −Y direction. As deposition continues, another change in direction is observed at the rounded section preceding segment C, where motion shifts to the +X direction. Along segment C, the force decreases as the trajectory exits the corner, returning to approximately the same range of values as observed for segment A. Throughout the entire toolpath, Fz oscillates within a range of approximately 1 N, with peaks and directional changes occurring at the rounded sections. Approaching segment S, the Z-axis force begins to increase, passing through segment T, and then starts to decrease after the rounded section preceding bead U. The increase in Fz observed along the side corresponding to segments B, C, T, and S indicates that the build platform is higher on this side than on the opposite side. The same forces behavior of the first layer is observed for the second one, although with lower force magnitudes, as the layer height is increased to 3 mm for the rest of the fabrication process.

As mentioned previously, the forces curves exhibited a progressive decrease in the measured forces after a certain period of time. Following data analysis and correlation between the recorded measurements, fabrication videos, time stamps, and sensor data acquisition, this decrease was observed to become more pronounced starting from the third layer (Fig. 8), where the signature of the different stages within a single layer disappears. In contrast, for the first two layers, the signatures of the main stages of a layer's toolpath are clearly identifiable. This absence of trajectory-related data persists for all layers beyond the second layer.

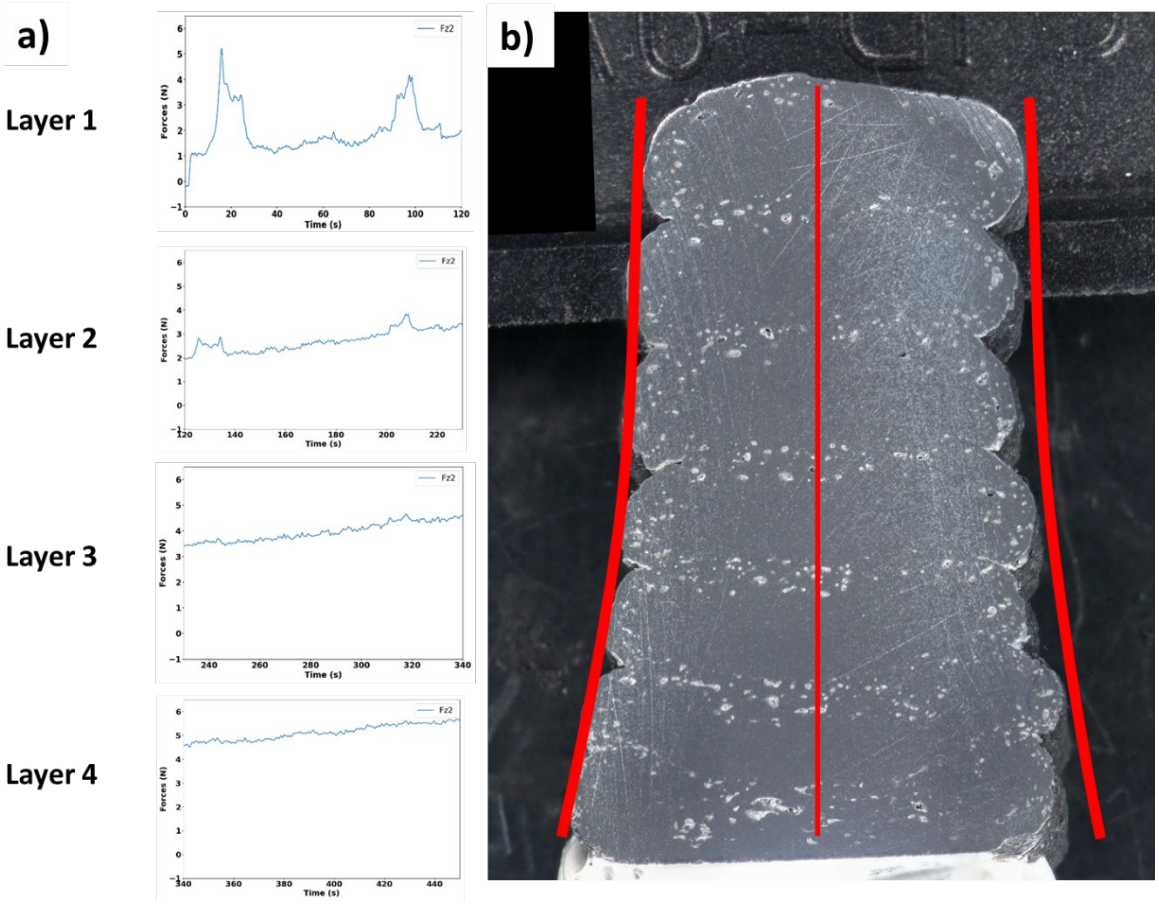

Fig. 8. a) Forces curves measured in Z-axis (Fz) of different layers and b) layers captured on the microscope.

Conclusions and Perspectives

The forces applied to the deposited material were quantified during the extrusion of pellets by robotic additive manufacturing. A six-component force sensor was used, allowing measurement of forces and moments along the three directions (X, Y, and Z). Following data acquisition, the results allowed understanding of force variations throughout the fabrication cycle and their correlation with the different stages of the manufacturing process. These measurements aim to facilitate the detection of manufacturing defects through unexpected force variations and to relate these observations to the final mechanical properties of the fabricated parts. A single layer curve was explained with the corresponding peaks of each segment of the trajectory. It was found that at rounds there are peaks in Z forces due to the fact that there is a slight accumulation of material, as the robot's travel speed decreases while the material flow rate remains constant. This therefore results in higher applied forces. Consequently, it was observed that from the third layer onward, forces along the Z direction were almost no longer detectable. Results were further supported by a thermal and microscopic analysis of the deposited layers.

The next steps will involve expanding the current study with additional fabrications and force measurements performed at a 45° angle. A comprehensive experimental protocol will be established to ensure data consistency and reproducibility. Further investigations will focus on dimensional metrology, the design and fabrication of standardized test specimens, and a series of mechanical tests to evaluate the material's performance. In addition, more advanced thermal analyses will be conducted to better understand the influence of temperature on the manufacturing process and the properties of the resulting parts.

References

[1] R. Kumar, H. Mehdi, S. S. Bhati, M. Arunkumar, S. Mishra, and M. K. Lohumi, "A comprehensive review of advancements in additive manufacturing for 3D printed medical components using diverse materials," Discov. Mater., vol. 5, no. 1, p. 152, 2025, doi: 10.1007/s43939-025-00349-w.

[2] S. Ouassil, A. El Magri, H. R. Vanaei, and S. Vaudreuil, " Investigating the effect of printing conditions and annealing on the porosity and tensile behavior of 3D -printed polyetherimide material in Z -direction ," J. Appl. Polym. Sci., no. October, pp. 1–16, 2022, doi: 10.1002/app.53353.

[3] K. Clancy, S. Xie, and O. Onaizah, "Advances in 3D Printing Technologies for Fabricating Magnetic Soft Microrobots," Adv. Intell. Syst., vol. n/a, no. n/a, p. 2500051, Jul. 2025, doi: https://doi.org/10.1002/aisy.202500051.

[4] A. D. Toth, J. Padayachee, T. Mahlatji, and S. Vilakazi, "Report on case studies of additive manufacturing in the South African railway industry," Sci. African, vol. 16, 2022, doi: 10.1016/j.sciaf.2022.e01219.

[5] H. Amirahmadi et al., "Screw extrusion-based additive manufacturing of fiber-reinforced high-temperature thermoplastics," Iran. Polym. J., 2025, doi: 10.1007/s13726-025-01536-5.

[6] K. Mitchell et al., "Molten Embedded Writing of End-Use Thermoplastics for Engineering Applications," ACS Appl. Mater. Interfaces, vol. 17, no. 50, pp. 68417–68430, Dec. 2025, doi: 10.1021/ACSAMI.5C16456/SUPPL_FILE/AM5C16456_SI_007.MP4.

[7] R. A. Nargis and D. A. Jack, "Fiber Orientation Quantification for Large Area Additively Manufactured Parts Using SEM Imaging," Polymers (Basel)., vol. 15, no. 13, p. 2871, Jun. 2023, doi: 10.3390/POLYM15132871.

[8] J. Sultana, M. M. Rahman, Y. Wang, A. Ahmed, and C. Xiaohu, “Influences of 3D printing parameters on the mechanical properties of wood PLA filament: an experimental analysis by Taguchi method,” Prog. Addit. Manuf., vol. 9, no. 4, pp. 1239–1251, 2024, doi: 10.1007/s40964-023-00516-6.

[9] A. El Magri, S. E. Ouassil, and S. Vaudreuil, “Effects of printing parameters on the tensile behavior of 3D-printed acrylonitrile styrene acrylate (ASA) material in Z direction,” Polym. Eng. Sci., vol. 62, no. 3, pp. 848–860, 2022, doi: 10.1002/pen.25891.

[10] M. Mencarelli, M. Sisella, L. Puggelli, B. Innocenti, and Y. Volpe, “Sensitivity Analysis of 3D Printing Parameters on Mechanical Properties of Fused Deposition Modeling-Printed Polylactic Acid Parts,” Appl. Mech., vol. 6, no. 1, Mar. 2025, doi: 10.3390/applmech6010017.

[11] H. Gaub, “Customization of mass-produced parts by combining injection molding and additive manufacturing with Industry 4.0 technologies,” Reinf. Plast., vol. 60, no. 6, pp. 401–404, Nov. 2016, doi: 10.1016/j.repl.2015.09.004.

[12] M. Mele, G. Campana, and G. Fumelli, “Environmental impact assessment of Arburg plastic freeforming additive manufacturing,” Sustain. Prod. Consum., vol. 28, pp. 405–418, Oct. 2021, doi: 10.1016/J.SPC.2021.06.012.

[13] S. Singamneni, A. Warnakula, D. A. Smith, and M. J. Le Guen, “Biopolymer Alternatives in Pellet Form for 3D Printing by Extrusion,” 3D Print. Addit. Manuf., vol. 6, no. 4, pp. 217–226, Aug. 2019, doi: 10.1089/3DP.2018.0152.

[14] M. Fabrizio, M. Strano, D. Farioli, and H. Giberti, “Extrusion Additive Manufacturing of PEI Pellets,” J. Manuf. Mater. Process. 2022, Vol. 6, Page 157, vol. 6, no. 6, p. 157, Dec. 2022, doi: 10.3390/JMMP6060157.

[15] F. Pignatelli and G. Percoco, “An application- and market-oriented review on large format additive manufacturing, focusing on polymer pellet-based 3D printing,” Progress in Additive Manufacturing, vol. 7, no. 6. Springer Science and Business Media Deutschland GmbH, pp. 1363–1377, Dec. 01, 2022. doi: 10.1007/s40964-022-00309-3.

[16] Y. P. Shaik, J. Schuster, A. Shaik, Y. P. Shaik, J. Schuster, and A. Shaik, “A Scientific Review on Various Pellet Extruders Used in 3D Printing FDM Processes,” vol. 8, no. 8, Jul. 2021, doi: https://doi.org/10.4236/oalib.1107698.

[17] S. Singamneni, D. Smith, M. J. LeGuen, and D. Truong, “Extrusion 3D Printing of Polybutyrate-Adipate-Terephthalate-Polymer Composites in the Pellet Form,” Polym. 2018, Vol. 10, Page 922, vol. 10, no. 8, p. 922, Aug. 2018, doi: 10.3390/POLYM10080922.

[18] P. Urhal, A. Weightman, C. Diver, and P. Bartolo, “Robot assisted additive manufacturing: A review,” Robot. Comput. Integr. Manuf., vol. 59, pp. 335–345, 2019, doi: https://doi.org/10.1016/j.rcim.2019.05.005.

[19] J. Lettori, R. Raffaeli, P. Bilancia, M. Peruzzini, and M. Pellicciari, “A review of geometry representation and processing methods for cartesian and multiaxial robot-based additive manufacturing,” Int. J. Adv. Manuf. Technol., vol. 123, no. 11, pp. 3767–3794, 2022, doi: 10.1007/s00170-022-10432-8.

[20] Prusa3d, “Types of printers and their differences,” https://help.prusa3d.com/article/types-of-printers-and-their-differences_112464, 2025.

[21] D. Moreno Nieto and S. I. Molina, “Large-format fused deposition additive manufacturing: a review,” Rapid Prototyping Journal, vol. 26, no. 5. Emerald Group Holdings Ltd., pp. 793–799, May 19, 2020. doi: 10.1108/RPJ-05-2018-0126.

[22] A. Oleff, B. Küster, M. Stonis, and L. Overmeyer, “Process monitoring for material extrusion additive manufacturing: a state-of-the-art review,” Prog. Addit. Manuf., vol. 6, no. 4, pp. 705–730, 2021, doi: 10.1007/s40964-021-00192-4.

[23] M. Barry, Y. Jacquet, F. Z. Kachkouch, and A. Perrot, “Instrumentation of the Extruder Nozzle Using Load Cells: Towards an In-Line Quality Control Device for 3D Printed Cement-Based Materials BT - Fourth RILEM International Conference on Concrete and Digital Fabrication,” 2024, pp. 142–149.

[24] I. Christodoulou, A. Trikkas, and A. Markopoulos, “Measurement and Analysis of Extrusion Forces in Filament-Based Additive Manufacturing Technologies Using ABS Filament,” Lect. Notes Mech. Eng., pp. 259–271, 2025, doi: 10.1007/978-3-031-83583-4_18.

[25] J. Dietz, P. Wüst, D. Spiehl, E. Dörsam, and A. Blaeser, “Force-based process monitoring in extrusion-based additive manufacturing,” Virtual Phys. Prototyp., vol. 20, no. 1, 2025, doi: 10.1080/17452759.2025.2567383.

[26] J. W. Kopatz, D. Reinholtz, A. W. Cook, A. S. Tappan, and A. M. Grillet, “Pressure-based process monitoring of direct-ink write material extrusion additive manufacturing,” Addit. Manuf., vol. 80, p. 103928, Jan. 2024, doi: 10.1016/J.ADDMA.2023.103928.

[27] W. De Backer, P. Sinkez, I. Chhabra, M. van Tooren, and A. P. Bergs, “In-process monitoring of continuous fiber additive manufacturing through force/torque sensing on the nozzle,” AIAA Scitech 2020 Forum, vol. 1 PartF, pp. 1–8, 2020, doi: 10.2514/6.2020-1632.

[28] S. Kasmi, G. Ginoux, S. Allaoui, S. Alix, and A. Sébastien, “Investigation of 3D printing strategy on the mechanical performance of coextruded continuous carbon fiber reinforced PETG,” PETG. J. Appl. Polym. Sci., vol. 138, no. 37, 2021, doi: 10.1002/app.50955ï.

[29] P. Zmuda Trzebiatowski, T. Królikowski, A. Ubowska, and K. Wilpiszewska, “Preparation and Properties of PETG Filament Modified with a Metallic Additive,” Materials (Basel)., vol. 18, no. 6, Mar. 2025, doi: 10.3390/ma18061203.